5464 J. Am. Chem. Soc. 1984, 106, 5464-5472

Synthesis and Characterization of Heterobimetallic Complexes Derived from (*o*-(Diphenylphosphino)benzoyl)pinacolone (HacacP). The Structure of $PtCl_2\{Cu(acacP)_2\}$

Debra A. Wrobleski,[1a] Cynthia S. Day,[1b] Bernard A. Goodman,*[1a,c] and Thomas B. Rauchfuss*[1a,d]

Contribution from the School of Chemical Sciences, University of Illinois, Urbana, Illinois 61801, and Crystalytics Company, Lincoln, Nebraska 68501. *Received October 17, 1983*

Abstract: The synthesis and characterization of heterobimetallic complexes of (*o*-(diphenylphosphino)benzoyl)pinacolone are described. Reaction of 2 equiv of HacacP with $MCl_2(COD)$ (M = Pd, Pt), $Rh_2Cl_2(CO)_4$, and $IrCl(CO)_2(p\text{-}H_2NC_6H_4CH_3)$ gave the metallo ligands of formulas $ML_2(HacacP)_2$ where ML_2 = *cis*-$PdCl_2$ and $PtCl_2$ and *trans*-Rh(CO)Cl and Ir(CO)Cl. The $ML_2(HacacP)_2$ metallo ligands undergo smooth metalation by cupric carboxylates giving the heterobimetallic complexes of the formula $ML_2\{Cu(acacP)_2\}$. The diamagnetic heterobimetallic complex $PtCl_2\{Ti(acacP)_2Cl_2\}$ was prepared from $TiCl_4$ and $PtCl_2(HacacP)_2$. On the basis of ^{31}P NMR, the Pt–Ti complex contains an unsymmetrical *cis*-$TiCl_2(acacP)_2$ subunit attached to a *cis*-$PtCl_2$ moiety. Treatment of $ZnEt_2$ with 2 equiv of HacacP followed by $IrCl(CO)_2(p\text{-}H_2NC_6H_4CH_3)$ gave *trans*-$IrCl(CO)\{Zn(acacP)_2\}$. The low-temperature ^{31}P NMR spectrum of the Ir–Zn complex established the predominance of an isomer featuring trans but nonequivalent phosphines. By IR spectroscopy, the Ir–Zn and Ir–Cu complexes are structurally similar as are the Pd–Cu and Pt–Cu compounds. The Pt–Cu complex was characterized by single-crystal X-ray crystallography. $PtCl_2\{Cu(acacP)_2\}\cdot 2CH_2Cl_2\cdot H_2O$ crystallizes in the centrosymmetric triclinic space group $P\bar{1}—C_i^1$ (no. 2) with a = 11.914 (6) Å, b = 11.646 (6) Å, c = 21.125 (10) Å, α = 102.34 (4)°, β = 103.71 (4)°, γ = 99.83°, and Z = 2. The empirically weighted full-matrix least-squares refinement converged to R_1 = 0.053 and R_2 = 0.065 for 8881 independent reflections having 2θ (Mo K$\bar{\alpha}$) < 55° and $I > 3\sigma(I)$. The molecule consists of square-planar $PtCl_2P_2$ and $Cu(\beta\text{-diketonate})_2$ subunits with a nonbonding Pt···Cu separation of 3.97 Å. Optical spectra of $IrCl(CO)\{Cu(acacP)_2\}$ exhibit an intense absorption at 960 nm that is not found in typical square-planar Ir(I) or Cu(II) model compounds. This band disappears upon treatment with SO_2, and the visible spectrum of $IrCl(CO)\{Cu(acacP)_2\}\cdot SO_2$ resembles that for a typical $Cu(\beta\text{-diketonate})_2$ chromophore. Similarly EPR studies indicate that the Pt–Cu and Ir–Cu–SO_2 complexes consist of axially symmetric Cu moieties. EPR studies on $IrCl(CO)\{Cu(acacP)_2\}$ indicate that it contains a low-symmetry Cu site (g_x = 2.038, 2.146, 2.278) and a relatively small isotropic hyperfine splitting, both of which are consistent with the presence of a tetrahedrally distorted $Cu(\beta\text{-diketonate})_2$ unit. These data are consistent with the formation of an enolate bridge between iridium and copper centers.

Introduction

The preparation of compounds that contain two different metals is currently being pursued in several laboratories. This topic receives considerable attention because heterometallic compounds are widely perceived to be of both theoretical and practical value. It is within the realm of coordination chemistry that heterobimetallic compounds display particularly novel physical and spectroscopic properties.[1,2] The distinctive catalytic properties of those metalloenzymes that contain two different metals, e.g., nitrogenase and cytochrome *c* oxidase, serve as a continual remainder of the potential value of synthetic heterobimetallics.[3] Of greatest challenge to and value for synthesis are those complexes wherein one or both of the metals is capable for substrate binding.[4]

A particularly versatile approach to the development of heterobimetallic chemistry employs multidentate ligands capable of assembling and stabilizing various combinations of metals.[5] For example, the derivatives of the Schiff base type ligands, e.g., $((fsa)_2en)^{4-}$, have received considerable attention particularly from the perspective of magnetic and spectroscopic properties.[2,6] In general such compartmentalized ligands feature hard nitrogen and oxygen donors that bind well to many higher valent, first-row transition-metal ions but are not well and suited for the platinum metals. Interest in the lower valent platinum metal-containing heterobimetallics derives from the anticipation that such species may prove reactive yet spectroscopically tractable. With this goal in mind, the unsymmetrical ligand (*o*-(diphenylphosphino)benzoyl)pinacolone,[7] abbreviated HacacP, emerges as being ideally suited for the preparation of heterobimetalic complexes featuring

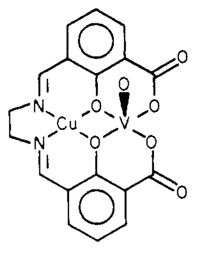

$CuV(O)((fsa)_2en)$

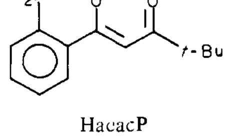

HacacP

---

[1] (a) University of Illinois. (b) Crystalytics Company. (c) On leave from Macaulay Institute for Soil Research, Craigiebuckler, Aberdeen, Scotland. (d) Fellow of A. P. Sloan and Camille and Henry Dreyfus Foundations.

[2] (a) Spiro, C. L.; Lambert, S. L.; Smith, T. J.; Duesler, E. N.; Gagné, R. R.; Hendrickson, D. N. *Inorg. Chem.* **1981**, *20*, 1229. (b) Gagné, R. R.; Spiro, C. L.; Smith, T. J.; Hamann, C. A. Thies, W. R.; Shiemke, A. K. *J. Am. Chem. Soc.* **1981**, *14*, 4073.

[3] (a) Ibers, J. A.; Holm, R. H. *Science (Washington, DC)* **1980**, *209*, 223-35. (b) Ochiai, E. "Bioinorganic Chemistry"; Allyn and Bacon, Inc.: Boston, MA 1977; Chapter 9, p 246.

[4] (a) Powell, J.; Gregg, M.; Kuksis, A.; Meindl, P. *J. Am. Chem. Soc.* **1983**, *105*, 1064-65. (b) Powell, J.; May, C. J. *Ibid.* **1982**, *104*, 2636-37. (c) Collman, J. P.; Bencosme, C. S.; Durand, R. R., Jr.; Kreh, R. P.; Anson, F. C. *Ibid.* **1983**, *105*, 2699.

[5] (a) Groh, S. E. *Isr. J. Chem.* **1976/1977**, *15*, 277-307. (b) Glick, M. D.; Lintvedt, R. L. *Prog. Inorg. Chem.* **1976**, *21*, 233. (c) Casellato, U.; Vigato, P. A.; Fenton, D. E.; Vidali, M. *Chem. Soc. Rev.* **1979**, *8*, 199-220.

[6] Kahn, O.; Claude, R.; Coudanne, H. *Nouv. J. Chim.* **1980**, *4*, 167-72.

[7] Wrobleski, D. A.; Rauchfuss, T. B.; Rheingold, A. L.; Lewis, K. A. *Inorg. Chem.*, in press.

0002-7863/84/1506-5464$01.50/0

both hard and soft metals. By design HacacP is sufficiently flexible to bridge two coordination polyhedra yet sufficiently rigid to preclude its functioning as a tridentate P, O, O chelating agent.

In this paper we expand upon our preliminary report[8] by describing syntheses of heterobimetallic derivatives of HacacP. While the synthetic details are specific for HacacP, the overall strategies employed appear to be of some generality. We also describe in some detail the spectroscopic methodologies used to evaluate intermetallic interactions in these derivatives.

Experimental Section

Materials and Methods. All compounds described herein are air stable in the solid state with the exception of $\mathrm{PtCl_2\{Ti(acacP)_2Cl_2\}}$ which is moisture sensitive. Syntheses were routinely conducted by using Schlenk techniques. Tetrahydrofuran (THF) and toluene were freshly distilled under nitrogen from sodium benzophenone ketyl and sodium, respectively. All other reagent grade chemicals were used without further purification. The following compounds were prepared according to published procedures: $\mathrm{PtCl_2(COD)}$[9] (COD = 1,5-cyclooctadiene), $\mathrm{PdCl_2(COD)}$,[10] $\mathrm{IrCl(CO)_2(}p\mathrm{\text{-}NH_2C_6H_4Me)}$,[11] and (*o*-(diphenylphosphino)benzoyl)pinacolone[7] (HacacP). Cupric heptanoate was prepared from cupric acetate and heptanoic acid.

The following instruments were used in this work: IR, Perkin-Elmer 599B; FTIR, Nicolet 5-MX; UV–vis, Varian Cary 219; UV–vis–near-IR, Varian 2300; 90-MHz ^{1}H NMR, Varian EM-390 (with internal frequency lock); 40.5-MHz ^{31}P{^{1}H} NMR, Varian XL-100 (internal ^{2}H frequency lock, positive δ down-field of external standard 85% $\mathrm{H_3PO_4}$); 101.3-MHz ^{31}P{^{1}H} NMR, NSF 250 system with a 5.87T Oxford Instruments magnet and a Nicolet NIC-80 data system (unlocked, positive δ downfield of external standard 85% $\mathrm{H_3PO_4}$); X-band EPR, Varian E 102 microwave bridge with a Varian E9 console/magnet equipped with a Varian gas flow cell for $\mathrm{CH_2Cl_2}$/toluene (1:1) glasses (calibration standard DPPH, 9.1 GHz); Q-band EPR, Varian E 101 microwave bridge with a Varian E12 console/magnet equipped with a gas flow Dewar for $\mathrm{CH_2Cl_2}$/toluene (1:1) glasses (calibration standard DPPH, 35.2 GHz). Simulations of the EPR spectra were performed by using "Program POWD" by R. L. Belford, A. M. Maurice, and M. Nilges.[12,13] A four-point Gauss-point integration procedure was used, and only the electronic *g* and hyperfine terms were considered for the simulation procedure. For ease of simulation the ^{63}Cu-enriched complexes were synthesized from $\mathrm{^{63}Cu(OAc)_2{\cdot}H_2O}$ that was prepared by treatment of ^{63}CuO with hot glacial acetic acid. Field desorption (FD) and fast atom bombardment (FAB) mass spectra were measured as a service on Varian 731 spectrometer and ZAB-HF (VG instruments), respectively, at the Mass Spectrometry Laboratory. Elemental analysis data and osmometric weight measurements were obtained from the University of Illinois Microanalytical Laboratory.

***cis*-$\mathbf{PtCl_2(HacacP)_2}$.** A solution of $\mathrm{PtCl_2(COD)}$ (186 mg, 0.5 mmol) and HacacP (388 mg, 1.0 mmol) in $\mathrm{CH_2Cl_2}$ (30 mL) was stirred for 30 min. Addition of hexane (15 mL) and concentration to two-thirds volume afforded pale yellow crystals in 84% yield (435.2 mg).

***cis*-$\mathbf{PdCl_2(HacacP)_2}$.** To a solution of $\mathrm{PdCl_2(COD)}$ (142.6 mg, 0.5 mmol) in $\mathrm{CH_2Cl_2}$ (50 mL) was added HacacP (388 mg, 0.1 mmol) in $\mathrm{CH_2Cl_2}$ (10 mL). Addition of hexane (20 mL) and concentration of the yellow-orange solution to approximately one-half volume gave a yellow solid. Recrystallization of the crude product from $\mathrm{CH_2Cl_2}$ (10 mL) by the addition of hexane (25 mL) gave yellow crystals in 92% yield (437.6 mg).

***trans*-$\mathbf{IrCl(CO)(HacacP)_2}$.** A solution of HacacP (298 mg, 0.768 mmol) in THF (10 mL) was added dropwise to $\mathrm{IrCl(CO)_2(}p\text{-}\mathrm{toluidine)}$ (150 mg, 0.384 mmol) in THF (40 mL). The resulting brown solution was stirred for 30 min, diluted with hexane (10 mL), concentrated to approximately one-half volume, and filtered through Celite. The addition of more hexane (~5 mL) and further concentration afforded yellow crystals in 58.5% yield (229.4 mg).

***trans*-$\mathbf{RhCl(CO)(HacacP)_2}$.** A $\mathrm{CH_2Cl_2}$ solution (5 mL) of HacacP (388 mg, 1.0 mmol) was added to a $\mathrm{CH_2Cl_2}$ solution (5 mL) of $\mathrm{Rh_2Cl_2(CO)_4}$ (97.2 mg, 0.25 mmol). Addition of hexane to the orange solution followed by concentration afforded yellow crystals, which become orange upon drying, in 90% yield (426 mg).

$\mathbf{PtCl_2\{Cu(acacP)_2\}}$. A solution of *cis*-$\mathrm{PtCl_2(HacacP)_2}$ (350 mg, 0.34 mmol) in methanol (175 mL) was added to cupric heptonoate (67.2 mg, 0.34 mmol) in methanol (75 mL). After the mixture was stirred for 1 h, the solvent was removed. The product was obtained as green crystals in 95% yield (351 mg) from $\mathrm{CH_2Cl_2}$ solution by the addition of hexane. FDMS: m/z 1068 ($(\mathrm{M-Cl})^+$), 1033 ($(\mathrm{M-Cl_2})^+$).

$\mathbf{PtCl_2\{Ti(acacP)_2Cl_2\}}$. To a solution of *cis*-$\mathrm{PtCl_2(HAcacP)_2}$ (200 mg, 0.192 mmol) in THF (50 mL) was added a 0.565 M toluene solution of $\mathrm{TiCl_4}$ (340 μL, 0.192 mmol) that was standardized by quenching an aliquot with absolute ethanol followed by titration with 0.1 M NaOH. The resulting orange solution was purged with $\mathrm{N_2}$ and heated to reflux for 0.5 h to give a deep red-orange solution. After removal of the solvent in vacuo, the yellow-orange product was reprecipitated from $\mathrm{CH_2Cl_2}$ (8 mL) by the addition of hexane (20 mL) affording 77% yield (172 mg). FDMS: m/z 1157 ($\mathrm{M^+}$).

$\mathbf{PdCl_2\{Cu(acacP)_2\}}$. A solution of *cis*-$\mathrm{PdCl_2(HacacP)_2}$ (80 mg, 0.084 mmol) in $\mathrm{CH_2Cl_2}$ (15 mL) and MeOH (15 mL) was added dropwise to a cupric heptanoate (27 mg, 0.084 mmol) in MeOH (10 mL). After being stirred 0.5 h, the solution became dark green. After solvent removal, crystallization from $\mathrm{CH_2Cl_2}$ (5 mL) and hexane (10 mL) gave olive green crystals in 47% yield (40 mg). FAB Ms: m/z 945 ($(\mathrm{M-Cl_2})^+$).

$\mathbf{IrCl(CO)\{Cu(acacP)_2\}}$. A solution of *trans*-$\mathrm{IrCl(CO)(HacacP)_2}$ (100 mg, 0.098 mmol) in THF (25 mL) was added dropwise to cupric heptanoate (31.5 mg, 0.098 mmol) in THF. The green solution changed to red-brown after 10 min. Addition of hexane and concentration gave dark red crystalline product in 73% yield (78.2 mg). FDMS: m/z 1090 ($\mathrm{M^+}$), 1058 ($(\mathrm{M-Cl})^+$); M_r(benzene) 1046 (calcd 1093).

$\mathbf{[IrCl(CO)\{Cu(acacP)_2\}SO_2]}$. A solution of $\mathrm{IrCl(CO)\{Cu(acacP)_2\}}$ (50 mg, 0.046 mmol) in $\mathrm{CH_2Cl_2}$ (20 mL) was stirred while a slow stream of $\mathrm{SO_2}$ was passed through the solution resulting in a color change to green. Addition of hexane (10 mL) and concentration under a stream of $\mathrm{N_2}$ and $\mathrm{SO_2}$ gave a green precipitate (35.6 mg, 67% yield) that was collected and dried under a slow stream of $\mathrm{SO_2}$.

$\mathbf{IrCl(CO)\{Zn(acacP)_2\}}$. To a solution of HacacP (388 mg, 1 mmol) was added $\mathrm{ZnEt_2}$ (600 μL, 13% by weight toluene solution, 0.5 mmol). After the solution was stirred for 1 h, the solvent was removed in vacuo. The $\mathrm{Zn(acacP)_2}$ (0.5 mmol) was dissolved in $\mathrm{CH_2Cl_2}$ (10 mL) and added dropwise to a solution of $\mathrm{IrCl(CO)_2(}p\text{-}\mathrm{toluidine)}$ (195.3 mg, 0.5 mmol) in $\mathrm{CH_2Cl_2}$ (20 mL). The dark purple solution lightened to an amber color over the course of 5.5 h. Addition of hexane (~20 mL) and concentration gave a 49% yield (266.6 mg) of yellow crystals. FDMS: m/z 1066 $(\mathrm{M-CO})^+$, 1031 $(\mathrm{M-(CO)(Cl)})^+$.

$\mathbf{[IrCl(CO)\{Zn(acacP)_2\}SO_2]}$. Green solutions of the product were generated as described above for $\mathrm{[IrCl(CO)\{Cu(acacP)_2\}SO_2]}$ and used in situ. The product was not isolated as a solid.

X-ray Crystallographic Study of $\mathbf{PtCl_2\{Cu(acacP)_2\}{\cdot}2CH_2Cl_2{\cdot}H_2O}$. Crystals of $\mathrm{PtCl_2\{Cu(acacP)_2\}{\cdot}2CH_2Cl_2{\cdot}H_2O}$, suitable for X-ray diffraction studies, were grown from $\mathrm{CH_2Cl_2}$/hexane in air at room temperature. The compound crystallizes in the centrosymmetric triclinic space group $P\bar{1}$—C_i^1 (No. 2)[14] with $a = 11.914\ (6)$ Å, $b = 11.646\ (6)$ Å, $c = 21.125\ (10)$ Å, $\alpha = 102.34\ (4)°$, $\beta = 103.71\ (4)°$, $\gamma = 99.83\ (4)°$, and $Z = 2$ ($d_{\text{calcd}} = 1.59$ g cm^{-3} and μ_a(Mo K$\bar{\alpha}$)[15a] = 3.52 mm^{-1}). Intensity measurements were made on a computer-controlled Nicolet P$\bar{1}$ autodiffractometer using full 1.1° wide ω scans, graphite-monochromated Mo K $\bar{\alpha}$ radiation, and nearly cube-shaped crystal, 0.75 mm on an edge, that was cut from a larger single crystal and sealed with mother liquor in a thin-walled glass capillary. A total of 12 435 independent reflections having 2θ(Mo K$\bar{\alpha}$) < 55° were measured in two concentric shells of increasing 2θ. A scanning rate of 6.0°/min was employed for reflections having 2θ(Mo K$\bar{\alpha}$) < 43° and 4.0°/min for the remaining reflections. The scan for each reflection was between ω settings of 0.55° above and below the calculated K$\bar{\alpha}$ ($\lambda = 0.710\,73$ Å) doublet value. Counts were accumulated for 19 equal (time) intervals during each scan, and those 13 contiguous intervals that had the highest single accumulated count as their midpoint were used to calculate the net intensity from scanning. Background counts, each lasting for one-fourth the total time used for the net scan (13/19 of the total scan time), were measured at ω settings 1.1° above and below the calculated K_2 doublet value for each reflection. The intensities were reduced to relative squared amplitudes, $|F_o|^2$, by means of standard Lorentz and polarization corrections.

The Pt atom was located from a Patterson synthesis, and the remaining non-hydrogen atoms were located from a difference Fourier

---

[8] Wrobleski, D. A.; Rauchfuss, T. B. *J. Am. Chem. Soc.* **1982**, *104*, 2314–16.

[9] McDermott, J. X.; White, J. F.; Whitesides, G. M. *J. Am. Chem. Soc.* **1976**, *98*, 6521–28.

[10] Drew, D.; Doyle, J. R. *Inorg. Synth.* **1972**, *13*, 47–55.

[11] Klabunde, U. *Inorg. Synth.* **1974**, *15*, 82–4.

[12] Maurice, A. M.; Belford, R. L.; Goldberg, I. B.; Christe, K. O. *J. Am. Chem. Soc.* **1983**, *105*, 3799.

[13] Nilges, M. J.; Ph.D. Dissertation, University of Illinois, Urbana, IL, 1979.

[14] "International Tables for X-ray Crystallography"; Kynoch Press: Birmingham, England, 1969; Vol. I, p 75.

[15] (a) "International Tables for X-ray Crystallography"; Kynoch Press: Birmingham, England, 1974; Vol. IV, pp. 55–66. (b) *Ibid.*, pp 99–101. (c) *Ibid.*, pp 149–50.

Table I. Atomic Coordinates for Non-Hydrogen Atoms in Crystalline $PtCuCl_2P_2O_4C_{50}H_{48}\cdot 2CH_2Cl_2\cdot H_2O$[a]

atom type[b]	fractional coordinates		
	x	y	z
Pt	-0.03601 (3)	0.17411 (3)	0.17988 (1)
Cu	-0.10380 (8)	0.25129 (8)	0.35714 (4)
Cl_a	0.1455 (2)	0.3130 (2)	0.1997 (1)
Cl_b	0.0752 (2)	0.0237 (2)	0.1769 (1)
P_a	-0.1220 (2)	0.3310 (2)	0.1679 (1)
P_b	-0.1907 (2)	0.0142 (2)	0.1638 (1)
O_{a1}	-0.0585 (5)	0.3590 (5)	0.3066 (2)
O_{a2}	0.0385 (5)	0.3139 (5)	0.4278 (3)
O_{b1}	-0.2299 (4)	0.1703 (5)	0.2794 (2)
O_{b2}	-0.1706 (5)	0.1730 (5)	0.4141 (3)
C_{a1}	-0.0318 (7)	0.4863 (7)	0.2110 (4)
C_{a2}	0.0350 (7)	0.5271 (7)	0.2807 (4)
C_{a3}	0.0961 (8)	0.6475 (8)	0.3071 (4)
C_{a4}	0.0955 (8)	0.7302 (8)	0.2681 (5)
C_{a5}	0.0327 (9)	0.6914 (8)	0.2004 (5)
C_{a6}	-0.0290 (9)	0.5705 (8)	0.1728 (5)
C_{a7}	0.0349 (6)	0.4448 (7)	0.3259 (4)
C_{a8}	0.1271 (7)	0.4665 (7)	0.3846 (4)
C_{a9}	0.1231 (7)	0.4023 (7)	0.4334 (4)
C_{a10}	0.2239 (8)	0.4360 (8)	0.4998 (4)
C_{a11}	-0.1466 (8)	0.3289 (8)	0.0778 (4)
C_{a12}	-0.2367 (10)	0.3788 (9)	0.0437 (5)
C_{a13}	-0.2527 (11)	0.3730 (10)	-0.0249 (5)
C_{a14}	-0.1799 (11)	0.3184 (12)	-0.0587 (5)
C_{a15}	-0.0938 (12)	0.2679 (13)	-0.0258 (5)
C_{a16}	-0.0765 (9)	0.2743 (10)	0.0423 (4)
C_{a21}	-0.2677 (7)	0.3358 (7)	0.1799 (4)
C_{a22}	-0.2820 (8)	0.4180 (9)	0.2344 (5)
C_{a23}	-0.3968 (10)	0.4175 (11)	0.2409 (6)
C_{a24}	-0.4960 (9)	0.3395 (10)	0.1915 (7)
C_{a25}	-0.4818 (8)	0.2621 (9)	0.1365 (6)
C_{a26}	-0.3693 (8)	0.2591 (8)	0.1304 (5)
C_{am1}	0.3425 (11)	0.5051 (18)	0.4948 (7)
C_{am2}	0.2470 (15)	0.3222 (13)	0.5195 (8)
C_{am3}	0.1798 (14)	0.5166 (20)	0.5503 (6)
C_{b1}	-0.3519 (6)	0.0068 (7)	0.1524 (3)
C_{b2}	-0.3994 (6)	0.0332 (7)	0.2067 (3)
C_{b3}	-0.5226 (7)	0.0087 (8)	0.1972 (4)
C_{b4}	-0.6002 (7)	-0.0383 (9)	0.1326 (5)
C_{b5}	-0.5551 (7)	-0.0637 (9)	0.0775 (4)
C_{b6}	-0.4317 (7)	-0.0430 (8)	0.0877 (4)
C_{b7}	-0.3187 (6)	0.0880 (7)	0.2763 (3)
C_{b8}	-0.3448 (7)	0.0507 (8)	0.3312 (4)
C_{b9}	-0.2668 (7)	0.0925 (8)	0.3970 (4)
C_{b10}	-0.2949 (8)	0.0439 (8)	0.4546 (4)
C_{b11}	-0.1965 (7)	-0.0940 (8)	0.0857 (4)
C_{b12}	-0.1824 (8)	-0.0455 (10)	0.0316 (4)
C_{b13}	-0.1870 (9)	-0.1235 (11)	-0.0305 (5)
C_{b14}	-0.2073 (10)	-0.2455 (13)	-0.0370 (5)
C_{b15}	-0.2190 (14)	-0.2915 (12)	0.0160 (7)
C_{b16}	-0.2124 (11)	-0.2160 (10)	0.0779 (5)
C_{b21}	-0.1650 (7)	-0.0649 (7)	0.2310 (4)
C_{b22}	-0.2473 (9)	-0.1690 (8)	0.2261 (5)
C_{b23}	-0.2304 (11)	-0.2277 (10)	0.2774 (7)
C_{b24}	-0.1308 (11)	-0.1779 (13)	0.3342 (6)
C_{b25}	-0.0493 (10)	-0.0723 (12)	0.3399 (5)
C_{b26}	-0.0663 (8)	-0.0160 (9)	0.2877 (4)
C_{bm1}	-0.3349 (15)	0.1444 (12)	0.4990 (6)
C_{bm2}	-0.3917 (10)	-0.0736 (11)	0.4308 (5)
C_{bm3}	-0.1790 (11)	0.0218 (14)	0.4964 (7)
Cl_{11}	0.4185 (5)	0.6159 (6)	0.3389 (3)
Cl_{12}	0.4142 (5)	0.7101 (7)	0.2256 (3)
Cl_{21}	0.4400 (4)	0.2771 (4)	0.3456 (3)
Cl_{22}	0.2985 (5)	0.0620 (5)	0.3535 (3)
C_1	0.3533 (13)	0.5938 (14)	0.2530 (9)
C_2	0.2974 (12)	0.1880 (13)	0.3221 (7)
O_w	0.4606 (11)	0.4566 (12)	-0.0323 (7)

[a] The numbers in parentheses are the estimated standard deviations in the last significant digit. [b] Atoms are labeled in agreement with Figure 1.

Table II. Selected Bond Distances (Å), Nonbonding Distances (Å), and Bond Angles (deg) in Crystalline $PtCuCl_2P_2O_4C_{50}H_{48}\cdot 2CH_2Cl_2\cdot H_2O$[a,b]

	Bond Lengths		
$Pt–Cl_a$	2.358 (2)	$Cu–O_{a1}$	1.904 (5)
$Pt–Cl_b$	2.370 (2)	$Cu–O_{a2}$	1.882 (6)
$Pt–P_a$	2.274 (2)	$Cu–O_{b1}$	1.879 (5)
$Pt–P_b$	2.291 (2)	$Cu–O_{b2}$	1.895 (6)
$Cl_a\cdots Cl_6$	3.233 (3)	$O_{a1}\cdots O_{a2}$	2.747 (7)
		$O_{b1}\cdots O_{b2}$	2.756 (7)
$P_a\cdots P_b$	3.621 (3)	$O_{a1}\cdots O_{b1}$	2.590 (8)
$Cl_a\cdots P_a$	3.151 (3)	$O_{a2}\cdots O_{b2}$	2.654 (9)
$Cl_b\cdots P_b$	3.094 (3)	$Pt\cdots Cu$	3.966 (1)
$P_a–C_{a1}$	1.851 (8)	$P_b–C_{b1}$	1.862 (8)
$P_a–C_{a11}$	1.848 (8)	$P_b–C_{b11}$	1.829 (8)
$P_a–C_{a21}$	1.821 (9)	$P_b–C_{b21}$	1.845 (8)
$O_{a1}–C_{a7}$	1.278 (10)	$O_{b1}–C_{b7}$	1.280 (10)
$O_{a2}–C_{a9}$	1.276 (10)	$O_{b2}–C_{b9}$	1.271 (11)
$C_{a2}–C_{a7}$	1.49 (1)	$C_{b2}–C_{b7}$	1.49 (1)
$C_{a7}–C_{a8}$	1.39 (1)	$C_{b7}–C_{b8}$	1.40 (1)
$C_{a8}–C_{a9}$	1.40 (1)	$C_{b8}–C_{b9}$	1.40 (1)
$C_{a9}–C_{a10}$	1.54 (1)	$C_{b9}–C_{b10}$	1.53 (1)
	Bond Angles		
Cl_aPtCl_b	86.29 (8)	$O_{a1}CuO_{a2}$	93.0 (3)
Cl_aPtP_a	85.70 (7)	$O_{b1}CuO_{b2}$	93.9 (3)
Cl_aPtP_b	169.32 (7)	$O_{a1}CuO_{b1}$	86.4 (2)
Cl_bPtP_a	168.03 (8)	$O_{a1}CuO_{b2}$	165.6 (3)
Cl_bPtP_b	83.19 (7)	$O_{a2}CuO_{b1}$	169.4 (3)
P_aPtP_b	104.98 (7)	$O_{a2}CuO_{b2}$	89.3 (3)
PtP_aC_{a1}	118.2 (3)	PtP_bC_{b1}	130.7 (3)
PtP_aC_{a11}	105.0 (3)	PtP_bC_{b11}	105.8 (3)
PtP_aC_{a21}	122.6 (3)	PtP_bC_{b21}	112.6 (3)
$CuO_{a1}C_{a7}$	126.2 (5)	$CuO_{b1}O_{b7}$	125.6 (5)
$CuO_{a2}C_{a9}$	127.5 (5)	$CuO_{b2}C_{b9}$	127.3 (6)
$O_{a1}C_{a7}C_{a2}$	113.6 (7)	$O_{b1}C_{b7}C_{b2}$	113.4 (6)
$O_{a1}C_{a7}C_{a8}$	125.2 (7)	$O_{b1}C_{b7}C_{b8}$	125.9 (7)
$C_{a2}C_{a7}C_{a8}$	121.2 (7)	$C_{b2}C_{b7}C_{b8}$	120.7 (7)
$C_{a7}C_{a8}C_{a9}$	123.2 (8)	$C_{b7}C_{b8}C_{b9}$	123.1 (8)
$O_{a2}C_{a9}C_{a8}$	124.5 (7)	$O_{b2}C_{b9}C_{b8}$	124.1 (8)
$O_{a2}C_{a9}C_{a10}$	114.6 (7)	$O_{b2}C_{b9}C_{b10}$	114.7 (7)
$C_{a8}C_{a9}C_{a10}$	120.9 (7)	$C_{b8}C_{b9}C_{b10}$	121.2 (8)

[a] The numbers in parentheses are the estimated standard deviations in the last significant digit. [b] Atoms are labeled in agreement with Figure 1.

synthesis. Full-matrix least-squares refinement of the 67 non-hydrogen atoms that incorporated unit weighting and anisotropic thermal parameters for all non-hydrogen atoms gave R_1(unweighted, based on F)[16] = 0.047 and R_2(weighted, based on F)[16] = 0.054 for 5291 independent reflections having $2\theta(\text{Mo K}\bar{\alpha}) < 43°$ and $I > 3\sigma(I)$. All structure factor calculations employed recent tabulations of atomic form factors[15b] and an anomalous dispersion correction[15c] to the scattering factor of the Pt, Cu, Cl, and P atoms. The final cycles of empirically weighted[17] full-matrix least-squares refinement converged to $R_1 = 0.053$ and $R_2 = 0.065$ for 8881 independent reflections having $2\theta(\text{Mo K}\bar{\alpha}) < 55°$ and $I > 3\sigma(I)$. Since a careful comparison of the final F_o and F_c values indicated the absence of extinction effects, extinction corrections were not made.

All calculations were performed on a Data General Eclipse S-200 computer with 64K and 16-bit words, a floating point processor for 32- and 64-bit arithmetic, and versions of the Nicolet E-XTL interactive software package as modified at Crystalytics Co.

Results and Discussion

Synthesis. Heterobimetallic bis(acacP) complexes can be prepared via either of two reaction sequences. The first method involves the insertion of the hard metal into the O_4 compartment followed by coordination of the pendant phosphine moieties to a second, soft metal ion. For the synthesis of cupric derivatives of HacacP this approach suffers from competitive oxidation of the phosphine by copper(II). An alternative approach to the synthesis of heterobimetallic derivatives of HacacP involves co-

---

(16) The R values are defined as $R_1 = \{\sum||F_o| - |F_c||/\sum|F_o|$ and $R_2 = \{\sum w(|F_o| - |F_c|)^2/\sum w|F_o{}^2\}^{1/2}$, where w is the weight given each reflection. The function minimized is $\sum w(|F_o| - K|F_c|)^2$, where K is the scale factor.

(17) Empirical weights were calculated from the equation $\sigma = \sum^3{}_0 a_n|F_o|^n = 3.02 - 6.64 \times 10^{-2}|F_o| + 9.99 \times 10^{-4}|F_o|^2 - 2.72 \times 10^{-6}|F_o|^3$, the a_n being the coefficients derived from the least-squares fitting of the curve $||F_o| - |F_c|| = \sum_0{}^3 a_n|F_o|^n$, where the F_c values were calculated from the fully refined model using unit weighting and an $I > 3\sigma(I)$ rejection criterion.

Table III. Analytical Data for New Compounds[a]

compd	C	H	P	Cl	M
cis-$PtCl_2(HacacP)_2$	57.61 (57.58)	4.81 (4.80)	6.18 (5.95)	6.95 (6.80)	
cis-$PdCl_2(HacacP)_2$	62.92 (62.94)	5.23 (5.24)		7.74 (7.44)	
trans-$IrCl(CO)(HacacP)_2$	58.87 (59.32)	4.87 (4.85)	6.27 (6.01)		
trans-$RhCl(CO)(HacacP)_2$	64.88 (64.95)	5.25 (5.31)			
$PtCl_2\{Cu(acacP)_2\}$	54.30 (54.37)	4.28 (4.35)	5.72 (5.62)		5.63 (Cu) (5.76)
$PtCl_2\{Ti(acacP)_2Cl_2\}$	51.88 (51.78)	4.31 (4.14)		11.92 (12.24)	
$PdCl_2\{Cu(acacP)_2\}$	58.86 (59.12)	4.77 (4.73)	6.31 (6.11)	7.32 (6.99)	6.21 (Cu) (6.26)
$IrCl(CO)\{Cu(acacP)_2\}$	56.13 (55.98)	4.63 (4.39)	5.25 (5.67)	3.54 (3.24)	5.81 (Cu) (5.81)
$[IrCl(CO)\{Cu(acacP)_2\}SO_2]$	52.31 (52.89)	3.99 (4.15)			
$IrCl(CO)\{Zn(acacP)_2\}$	56.34 (55.89)	4.67 (4.38)	5.82 (5.66)	3.44 (3.24)	5.98 (Zn) (5.97)

[a] Calculated values in parentheses.

Table IV. Infrared and UV–vis Spectroscopic Data for New Compounds

		IR,[h] cm^{-1}	
compd	λ, nm (ϵ, cm^{-1} M^{-1})	ν_{CO}(terminal)	$\nu_{CO,C=C}$(ligand)
HacacP	289 (14560)[a]		1607 (s), 1508 (s), 1557 (s)
cis-$PtCl_2(HacacP)_2$	295 (19700)[b]		1580 (s), 1560 (sh)
cis-$PdCl_2(HacacP)_2$	359 (11600), 322 (21500), 300 (23900)[b]		1603 (s), 1559 (m), 1481 (m)[e]
trans-$IrCl(CO)(HacacP)_2$	432 (667), 384 (3400), 290 (23500)[c]	1955 (vs), 1946 (vs) (1964[a])	1607 (s), 1567 (sh)
trans-$RhCl(CO)(HacacP)_2$		1956 (vs), 1944 (vs)	1601 (s), 1572 (sh), 1559 (m)
$PtCl_2\{Cu(acacP)_2\}$	688 (118), 318 (17400)[b]		1576 (m), 1551 (s), 1524 (s), 1499 (m)[f]
$PdCl_2\{Cu(acacP)_2\}$	702 (245), 336 (32700), 267.5 (290000)[b]		1572 (m), 1545 (s), 1520 (s), 1497 (s)[g]
$PtCl_2\{Ti(acacP)_2Cl_2\}$			1570 (m), 1534 (s), 1512 (vs), 1481 (m)
$IrCl(CO)\{Cu(acacP_2\}$	960 (507), 553 (245), 433.5 (2430), 341 (20100)	1970 (vs), 1962 (vs) (1973[a])	1584 (s), 1559 (m), 1501 (s), 1481 (sh)
$IrCl(CO)\{Zn(acacP)_2\}$	434 (sh, 966), 370.5 (15450), 336.5 (18700), 290 (20400)	1977 (vs), 1969 (vs) (1971[a])	1584 (sh), 1572 (s), 1555 (s), 1510 (s), 1489 (m)
$[IrCl(CO)(HacacP)_2SO_2]$		(2031[a])	
$[IrCl(CO)\{Cu(acacP)_2\}SO_2]$	638 (32)[c]	2049 (vs), 2037 (vs) (2031[a])	1566 (m), 1545 (s), 1524 (s), 1503 (s), 1196 (m),[d] 1051 (m)[d]
$[IrCl(CO)\{Zn(acacP)_2\}SO_2]$		2029[a]	

[a] CH_2Cl_2 solutions. [b] THF solutions. [c] Benzene solutions. [d] ν_{SO}. [e] 336 cm^{-1} ($\nu_{Pd\text{-}Cl}$). [f] 281 and 259 cm^{-1} ($\nu_{Cu\text{–}O}$), $\nu_{Pt\text{–}Cl}$). [g] 321 and 265 cm^{-1}. [h] Mineral oil mull.

Table V. NMR Spectroscopic Data for New Compounds[a]

	^1H NMR,[b] ppm				
compd	OH	aromatic	CH	*t*-Bu	$^{31}P\{^1H\}$ NMR,[c] ppm
HacacP	14.8 (br, s)	7.7–6.8 (m)	5.87 (s)	1.09 (s)	–9.0 (s)
cis-$PtCl_2(HacacP)_2$	15.48 (br, s)	8.23–6.70 (m)	5.27 (s)	1.05 (s)	15.2 (s, $^1J(^{195}Pt,^{31}P)$ = 4187 Hz)
cis-$PdCl_2(HacacP)_2$	15.70 (br, s)	7.97–7.20 (m)	6.10 (s)	1.20 (s)	21.6 (s)
trans-$IrCl(CO)(HacacP)_2$	15.78 (br, s)	7.95–7.19 (m)	6.02 (s)	1.03 (s)	24.9 (s)[d]
					21.0 (s)[e]
trans-$RhCl(CO)(HacacP)_2$	15.81 (br, s)	8.0–7.02 (m)	6.01 (s)	1.06 (s)	32.2 (d, $^1J(^{103}Rh,^{31}P)$ = 137 Hz)[f]
$PtCl_2\{Ti(acacP)_2Cl_2\}$		8.2–6.9 (m)	5.27 (s)	1.59 (s)	11.05 $^1J(^{195}Pt,^{31}P)$ = 3780 Hz)
				1.12 (s)	7.55 ($^1J(^{195}Pt,^{31}P)$ = 3920 Hz, $^2J(^{31}P,^{31}P)$ = 14 Hz)[g]
$IrCl(CO)\{Zn(acacP)_2\}$		7.8–6.85 (m)	6.17 (s)	1.08 (s)	23.6, 16.3 ($^2J(^{31}P,^{31}P)$ = 425 Hz)[h]
$[IrCl(CO)\{Zn(acacP)_2\}SO_2]$					9.4 (s), 10.4,[i] 6.8[i]

[a] All spectra were obtained as $CDCl_3$ solutions unless otherwise noted. [b] Positive δ downfield of internal tetramethylsilane. [c] Positive δ downfield of external standard 85% H_3PO_4 at 40.5 MHz unless otherwise noted. [d] Minor singlets at δ 26.85 and 25.9. [e] Spectrum obtained at 101.3 MHz with minor AB quartet at δ 24.2 and 20.4 ($^2J(^{31}P,^{31}P)$ = 382 Hz). [f] Minor signals at δ 35.2 and 34.4 ($^1J(^{103}Rh,^{31}P)$ = 137 Hz). [g] AB quartet. [h] AB quartet with a minor signal at δ 22.8 in toluene-d_8 solution at –70 °C. [i] With minor peaks at δ 21.9, 13.4, 11.4, 9.4, 9.0, and 6.6 at –65 °C.

ordination of the phosphine donors to a soft metal followed by metalation of the O_4 site.

Treatment of solutions of MCl_2(1,5-cyclooctadiene) (M = Pd, Pt) with 2 equiv of HacacP results in the formation of the pale yellow *cis*-$MCl_2(HacacP)_2$ complexes (eq 1). These species are

$$MCl_2(COD) + 2HacacP \rightarrow MCl_2(HacacP)_2 + COD \quad (1)$$
$$M = Pd, Pt$$

highly soluble, are easily crystallized, and exhibit the spectroscopic properties in accord with their proposed structures (vide infra). The compound *trans*-$IrCl(CO)(HacacP)_2$ was prepared from the reaction of $IrCl(CO)_2$(*p*-toluidine) with 2 equiv of HacacP (eq 2). This species is also easily handled and is more resistant to

$$IrCl(CO)_2(p\text{-toluidine}) + 2HacacP \rightarrow$$
$$trans\text{-}IrCl(CO)(HacacP)_2 + CO + p\text{-toluidine} \quad (2)$$

oxygenation than is Vaska's complex itself.[18] The IR spectra of the monometallic compounds reveal absorptions due to the β-diketone at 1607–1559 cm^{-1}, shifted very little from the free ligand, thereby substantiating monodentate, P-bound HacacP ligands.

The metallo ligands $ML_n(HacacP)_2$ (M = Pd, Pt, Ir) exhibit a low-field signal in their ^1H NMR spectra assignable to the hydrogen-bonded hydroxyl proton and a singlet at $\delta \simeq 6$ assigned to the methine proton (Table V). Upon P-coordination the *tert*-butyl resonance remains a singlet and shifts ca. 0.1 ppm. ^{31}P NMR spectroscopy reveals the expected "coordination chemical shifts" downfield from HacacP.[19] The value for $^1J(^{195}Pt,^{31}P)$ of 4187 Hz for $PtCl_2(HacacP)_2$ confirms its cis stereochemistry.[20]

---

(18) Vaska, L. *Acc. Chem. Res.* **1968**, *1*, 335–44 and references therein.

(19) Grim, S. O.; Keiter, R. L.; McFarlene, W. *Inorg. Chem.* **1967**, *6*, 1133–7.

(20) Pregosin, P. L.; Kunz, R. W. "^{31}P and ^{13}C NMR of Transition Metal Phosphine Complexes"; Diehl, P., Fluck, E., Kosfeld, R., Eds.; Springer-Verlag: New York, 1979; Vol. 16.

The stereochemistry for the palladium complex is difficult to assign with complete confidence. Palladium(II) characteristically forms *trans* phosphine complexes and the far-IR spectrum for $PdCl_2(HacacP)_2$ shows ν_{Pd-Cl} absorptions in the 370–335 cm^{-1} range like that for *trans*-$PdCl_2(PPh_3)_2$.[21] In the case of the iridium complex, ^{31}P NMR spectroscopy (40.5 MHz) revealed an unexpected complexity; three absorptions were observed in an 1:1:20 ratio. The analogous rhodium complex $RhCl(CO)(HacacP)_2$ shows a very similar pattern with each signal being split by coupling to ^{103}Rh. At highest field (101.3 MHz) the ^{31}P NMR spectrum for $IrCl(CO)(HacacP)_2$ consists of an intense resonance at 21.0 ppm an AB quartet pattern characterized by δ 24.2 and 20.4 and $^2J(^{31}P,^{31}P) = 382$ Hz. These absorptions are attributed to two rotational isomers, each of which is trans and one of which contains nonequivalent phosphorus atoms. This is analogous to observations by Shaw and co-workers[22] for related iridium compounds derived from bulky tertiary phosphines.

Conversion of these metallo ligands to their copper(II) derivatives is easily accomplished by their reaction with copper carboxylates. Because of its convenient solubility, cupric heptanoate was often employed (eq 3 and 4). The Pd–Cu and Pt–Cu complexes are emerald green both as solids and in solution while the Ir–Cu species is bright red. Upon addition of the second metal the IR absorptions due to the β-diketone shift to 1584–1501 cm^{-1}, ca. 20–40 cm^{-1} lower frequency. Similar frequency shifts have been noted for other β-diketonate complexes.[21] These paramagnetic species were formulated on the basis of combustion analysis, solution molecular weight determinations, and field desorption mass spectrometry. The far-IR spectra of $MCl_2\{Cu(acacP)_2\}$ for M = Pd and Pt are similar, suggesting that they both have the cis stereochemistry. This is an interesting point since chelation to copper appears to induce a trans to cis change in the coordination about the palladium center.

$$cis\text{-}MCl_2(HacacP)_2 + Cu(O_2CR)_2 \rightarrow MCl_2\{Cu(acacP)_2\} + 2RCO_2H \quad (3)$$

$$M = Pt,\ Pd$$

$$trans\text{-}IrCl(CO)(HacacP)_2 + Cu(O_2CR)_2 \rightarrow IrCl(CO)\{Cu(acacP)_2\} + 2RCO_2H \quad (4)$$

The diamagnetic complex $PtCl_2\{Ti(acacP)_2Cl_2\}$ was prepared from $PtCl_2(HacacP)_2$ and $TiCl_4$ (eq 5). Like $Ti(acac)_2Cl_2$ itself, the Pt–Ti complex is a red-orange, moisture-sensitive compound. NMR studies of the Pt–Ti complex have also proved to be useful in the assignment of its stereochemistry. The ^1H NMR spectrum shows two signals of equal intensity for the *tert*-butyl protons consistent with the formation of the unsymmetrical cis isomer shown. The $^{31}P\{^1H\}$ NMR spectrum at both 40.5 and 101.3 MHz consists of an AB quartet ($^2J(^{31}P,^{31}P) = 14$ MHz) centered at δ 11.05 and 7.55 with $^1J(^{31}P,^{195}Pt) = 3780$ and 3902 Hz, respectively, consistent with the *cis*-$PtCl_2P_2$ subunit.[20] Assignment of the 14-Hz splitting to the coupling of two nonequivalent phosphorus atoms was substantiated by a homonuclear phosphorus decoupling experiment: irradiation of the center of the doublet at δ 7.05 caused the doublet at δ 11.55 to collapse to a singlet.

$$cis\text{-}PtCl_2(HacacP)_2 + TiCl_4 \rightarrow PtCl_2\{Ti(acacP)_2Cl_2\} + 2HCl \quad (5)$$

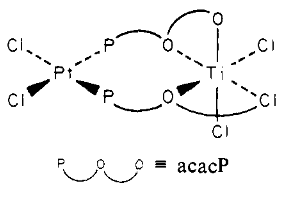

Another approach to the synthesis of heterobimetallic complexes is demonstrated through the preparation of $IrCl(CO)\{Zn(acacP)_2\}$. $Zn(acacP)_2$, prepared in situ from $ZnEt_2$ and 2 equiv of HacacP, was added to a CH_2Cl_2 solution of $IrCl(CO)_2$(*p*-toluidine) to give the yellow Ir–Zn complex (eq 6 and 7). This compound like the copper analogue is resistant to air oxidation.

$$ZnEt_2 + 2HacacP \rightarrow Zn(acacP)_2 + 2EtH \quad (6)$$

$$IrCl(CO)_2(p\text{-toluidine}) + Zn(acacP)_2 \rightarrow IrCl(CO)\{Zn(acacP)_2\} + CO + p\text{-toluidine} \quad (7)$$

While the carbonyl stretching frequency for solutions of *trans*-$IrCl(CO)(HacacP)_2$ is the same as for *trans*-$IrCl(CO)(PPh_3)_2$, the bimetallic complexes, Ir–Zn and Ir–Cu, are shifted ca. 10 cm^{-1} higher frequency. It is interesting to note that in the solid state both of these bimetallic complexes exhibit two ν_{CO} separated by ca. 7 cm^{-1} while in CH_2Cl_2 solution only one band is observed. The ^1H NMR spectrum of $IrCl(CO)\{Zn(acacP)_2\}$ consists of single resonances at δ 6.16 and 1.1 for the methine proton and the *tert*-butyl groups, respectively. The $^{31}P\{^1H\}$ NMR spectrum (40.5 MHz) shows a somewhat complex spectrum at 35 °C consisting of two broad absorptions with several sharp features. Upon cooling to low temperatures (−70 °C) the spectrum reveals a well-resolved AB quartet (δ 23.6, 16.3; $^2J(^{31}P,^{31}P) = 425$ Hz) and an additional small peak at δ 22.8. The nonequivalence of the phosphorus atoms of the major species is proposed to arise from a conformational isomer in which the ligands bridge the two metals in an unsymmetrical manner. The large coupling constant is completely consistent with assignment of a *trans* geometry about the iridium center,[23] *thereby confirming that this complex and by inference its Cu analogue contain trans spanning M(acacP)$_2$ diphosphine chelates.*

Conversion of the red Ir–Cu and yellow Ir–Zn complexes to their green sulfur dioxide adducts was achieved by purging solutions of the complex with SO_2 for several minutes (eq 8). This process is reversible as the starting materials are readily regenerated upon purging with nitrogen. The $[IrCl(CO)\{Cu(acacP)_2\}SO_2]$ complex was isolated as a solid and characterized by combustion analysis while the Ir–Zn SO_2 adduct was studied only in solution. The infrared carbonyl stretching frequencies for both of the iridium SO_2 complexes are shifted 10 cm^{-1} to higher frequency from Vaska's SO_2 adduct.[20] The geometry of SO_2 coordinated in these iridium complexes is assigned as an η^1-pyramidal geometry since the ν_{SO} absorptions at 1196 and 1051 cm^{-1} compare favorably with the data for related iridium SO_2 complexes that have been structurally characterized.[24] While the ^{31}P NMR spectrum of $[IrCl(CO)\{Zn(acacP)_2\}SO_2]$ consists of a singlet at ambient temperature, at −65 °C two major and several minor absorptions are observed. These data indicate the presence of several rapidly interconverting conformational isomers (vide supra) in solution.

$$IrCl(CO)\{M(acacP)_2\} + SO_2 \rightleftharpoons [IrCl(CO)\{M(acacP)_2\}SO_2] \quad (8)$$

$$M = Cu,\ Zn$$

Structure of $PtCl_2\{Cu(acacP)_2\}$. The structure of $PtCl_2\{Cu(acacP)_2\}$ was elucidated by a single-crystal X-ray diffraction study. The results (Figure 1) established that the two acacP ligands bridge approximately square-planar platinum and copper centers. The $PtCl_2$ and Cu(II) moieties are accommodated within the P_2 and O_4 compartments, respectively. The $PtCl_2P_2$ atoms are planar within 0.12 Å while the Cu(β-diketonate)$_2$ portion exhibits a greater distortion toward tetrahedral geometry with CuO_4 being coplanar within 0.21 Å. The planes defined by the coordination spheres of the two metals form a 67° angle. The Cu⋯Pt distance of 3.966 (1) Å confirms the absence of any bonding interaction

---

[21] Adams, D. M. "Metal-Ligand and Related Vibrations", Edward Arnold: London, 1967, p 12.

[22] Mann, B. E.; Masters, C.; Shaw, B. L.; Stainbank, R. E. *J. Chem. Soc., Dalton Trans.* **1971**, 1103–4.

[23] Bennett, M. A.; Johnson, R. N.; Tomkins, I. B. *J. Organomet. Chem.* **1977**, *133*, 231–71.

[24] Ryan, R. R.; Kubas, G. J.; Moody, D. C.; Eller, P. G. *Struct. Bonding (Berlin)* **1981**, *46*, 47–100.

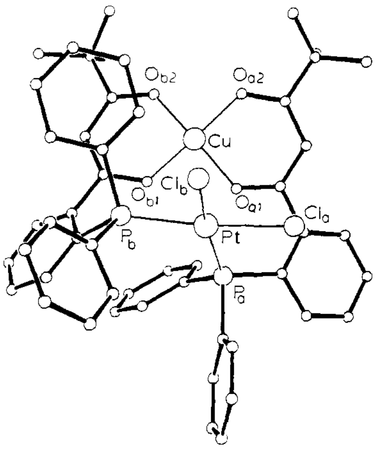

Figure 1. Ball and stick drawing for the non-hydrogen atoms of the $PtCl_2\{Cu(acacP)_2\}$ molecule. For purposes of clarity, metal atoms are represented by large open circles, chlorine and phosphorus atoms by medium-sized open circles, and carbon and oxygen atoms by small open circles.

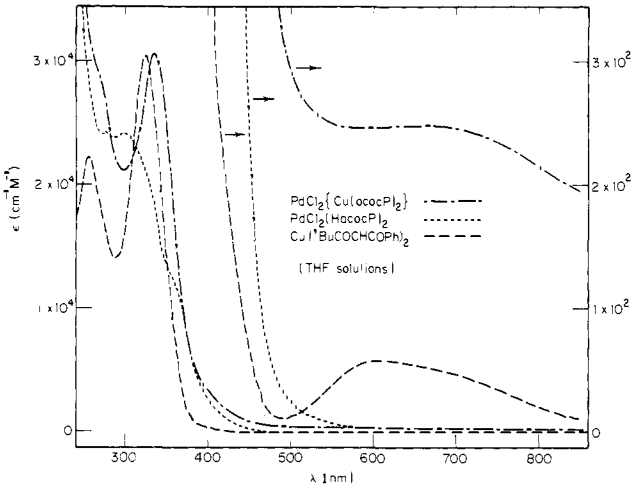

Figure 2. The UV–vis spectra of $PtCl_2\{Cu(acacP)_2\}$ (-—-) $PtCl_2(HacacP)_2$ (- - -), and $Cu(t\text{-}BuC(O)CHC(O)Ph)_2$ (– – –) in THF solutions.

since the sum of their covalent metallic radii is 2.67 Å.[25]

The Cu–O bond distances within the copper subunit are slightly shorter (0.04 Å) than those found for related species, e.g., *trans*-$Cu(CH_3C(O)CHC(O)Ph)_2$.[26] The bond distances in the platinum subunit are also unexceptional although the PPtP angle of 105° is ca. 7° larger than that found in other *cis*$PtCl_2L_2$ species (e.g., for L = PPh_3, PPtP = 97.8°[27]). Taken collectively the crystallographic analysis indicates that the $acacP^-$ ligand stabilizes the heterobimetallic unit in a relatively strain-free environment.

Optical Spectra of M{Cu(acacP)$_2$} Complexes. The visible absorption spectra for Cu(β-diketonate)$_2$ and their Lewis base adducts have been extensively studied.[28] While such spectra are generally poorly resolved, they can be shown to result from four, comparably intense, ligand field bands. It is these absorptions that are the most obvious indicators for Cu⋯M interactions in the compounds described in this work. The similarity of the visible spectra for the Pt–Cu (Figure 2) and Pd–Cu complexes to that for Cu(β-diketonate)$_2$ leads us to conclude that in solution there is little interaction between the metals. The visible spectral parameters of the Pt–Cu and Pd–Cu complexes largely appear to arise from the superimposition of the envelopes of Cu-localized d–d band on the trailing low-energy absorptions associated with the pale yellow *cis*-$MCl_2(HacacP)_2$ complexes.

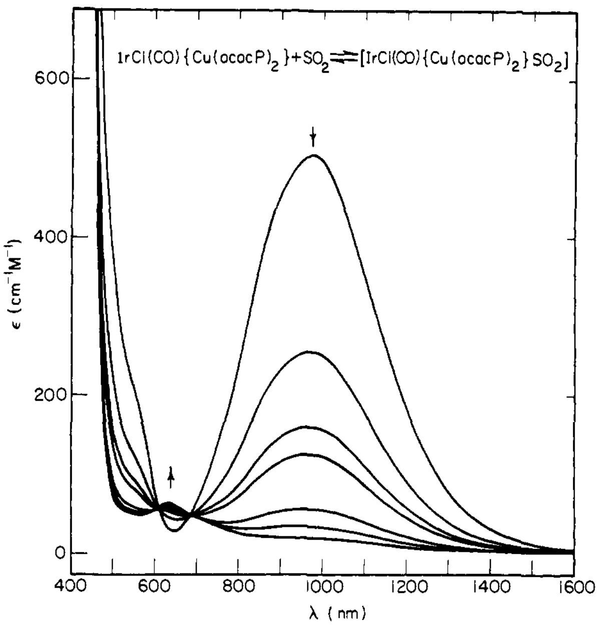

Figure 3. The vis-near-IR spectra of benzene solutions of $IrCl(CO)\{Cu(acacP)_2\}$ showing isosbestic behavior upon addition of SO_2.

In contrast to the Pt–Cu and Pd–Cu complexes, the optical spectrum of $IrCl(CO)\{Cu(acacP)_2\}$ features an intense low-energy absorption. This band at 960 nm (ϵ 507 cm^{-1} M^{-1}) obeys Beer's law and is absent for $IrCl(CO)\{Zn(acacP)_2\}$ although the similarity of the $IrCl(CO)(PR_3)_2$-localized bands[29] at 341 (ϵ 20 100 cm^{-1} M^{-1}) and 337 nm (18 700 cm^{-1} M^{-1}), for the Cu and Zn derivatives, respectively, supports assignment of very similar structures as does the IR data. The lower energy and high intensity of the 960-nm band contrasts with that for Cu(β-diketonates)$_2$ complexes and arises from the interaction of the Cu(II) and Ir(I) centers possibly mediated by an enolate bridge. This explanation is substantiated by our EPR studies (vide infra). Furthermore the binding of SO_2 by the iridium in $IrCl(CO)\{Cu(acacP)_2\}$ appears to disrupt the Cu⋯Ir interaction as evidenced by the fact that the visible spectrum of $[IrCl(CO)\{Cu(acacP)_2\}SO_2]$ (Figure 3) closely resembles that for an unperturbed Cu(β-diketonate)$_2$ chromophore. Thus there is a competition between Ir(I) functioning as a Lewis base toward SO_2 and Ir(I) functioning as a Lewis acid toward the Cu(β-diketonate)$_2$ subunit. We suggest that the latter interaction resembles the coordination of a methoxy group proposed to occur in *trans*-$IrCl(CO)(o\text{-}Ph_2PC_6H_4OCH_3)_2$.[30] The binding of SO_2 by $IrCl(CO)\{Cu(acacP)_2\}$ is reversible and exhibits isosbestic behavior (Figure 3). The UV region of the spectrum of $[IrCl(CO)\{Cu(acacP)_2\}SO_2]$ is very similar to that of $[IrCl(CO)\{Zn(acacP)_2\}SO_2]$ and $[IrCl(CO)(HacacP)_2SO_2]$.

The intense (ϵ 507 M^{-1} cm^{-1}) low-energy absorption at 960 nm for $[IrCl(CO)\{Cu(acacP)_2\}]$ is assigned to d–d transitions of a tetrahedrally distorted copper center. Previous work[31] on N-substituted salicylaldimine complexes of copper(II) has established that planar copper(II) complexes of N and O ligands are generally olive green [$\lambda_{max} \approx 600$ nm ($\epsilon \approx 100$ M^{-1} cm^{-1})] in color while tetrahedrally distorted derivatives are maroon [($\lambda_{max} \approx 750$ nm ($\epsilon \approx 2500$ M^{-1} cm^{-1})]. Examination of CPK models of the IrCu complex reveals that in order for the iridium(I) center to coordinate to an enolate oxygen, the copper(II) coordination sphere must distort.

EPR Spectra. The X-band EPR spectrum of $PtCl_2\{^{63}Cu(acacP)_2\}$ in a toluene–CH_2Cl_2 glass at 77 K (Figure 4) is indi-

---

[25] (a) Pauling, L. "The Nature of the Chemical Bond"; Cornell University Press: Ithaca, NY, 1960. (b) Royer, D. J. "Bonding Theory"; McGraw-Hill: New York, 1968.

[26] Hon, P.-K.; Pfluger, C. D.; Belford, R. L. *Inorg. Chem.* **1966**, *5*, 516–21.

[27] Anderson, G. K.; Clark, H. C.; Davies, J. A.; Ferguson, G.; Parrez, M. *J. Cryst. Spectrosc. Res.* **1982**, *12*, 449–58.

[28] Funck, L. L.; Ortolano, T. R. *Inorg. Chem.* **1968**, 567–73.

[29] Geoffroy, G. L.; Wrighton, M. S.; Hammond, G. S.; Gray, H. B. *J. Am. Chem. Soc.* **1974**, *96*, 3105–8.

[30] Miller, D. M.; Shaw, B. L. *J. Chem. Soc., Dalton Trans.* **1974**, 480–5.

[31] Sacconi, L.; Ciampolini, M. *J. Chem. Soc.* **1964**, 276–80.

Table VI. Calculated EPR Data for New Copper-Containing Bimetallic Complexes and Related Compounds[a]

compd	g_{soln}	$A(^{63}Cu)_{soln}$, MHz	g_x	g_y	g_z	$\|A_x\|$, MHz	$\|A_y\|$, MHz	$\|A_z\|$, MHz
$PtCl_2\{^{63}Cu(acacP)_2\}$	2.186	225	2.061	2.060	2.255	58	81	561
$IrCl(CO)\{^{63}Cu(acacP)_2\}$	2.176 2.134[c]	95–110[b] 204[c]	2.038	2.146	2.278	206	90–180[b]	314
$[IrCl(CO)\{^{63}Cu(acacP)_2\}SO_2]$[d]	2.125	207	2.057 2.057	2.056 2.058	2.059 2.059	68 68	82 49	540 547
$^{63}Cu(acac)_2$[e,f]	2.123	226	2.054	2.050	2.264	70	63	546
$^{63}Cu(bzac)_2\cdot EtOH$[e,g]	2.123	224	2.052	2.052	2.264	63	63	546

[a] All spectra were obtained as CH_2Cl_2/toluene (1:1) solutions (room temperature) or glasses (77 K) unless otherwise noted. [b] The uncertainty of these values is due to the inability to simulate the spectrum with a unique $|A_y|$ value. [c] Values obtained from 2-MeTHF solutions (room temperature). [d] The two sets of g and hyperfine values indicated here are by no means the unique solution but rather represent one set of data that fit the spectrum. [e] Powder spectrum of sample doped into a diamagnetic host. [f] Northern, T. M. Ph.D. Dissertation, University of Illinois, Urbana, IL, 1976. [g] Belford, R. L.; Duan, D. C. *J. Magn. Reson.* **1978**, *29*, 293–307.

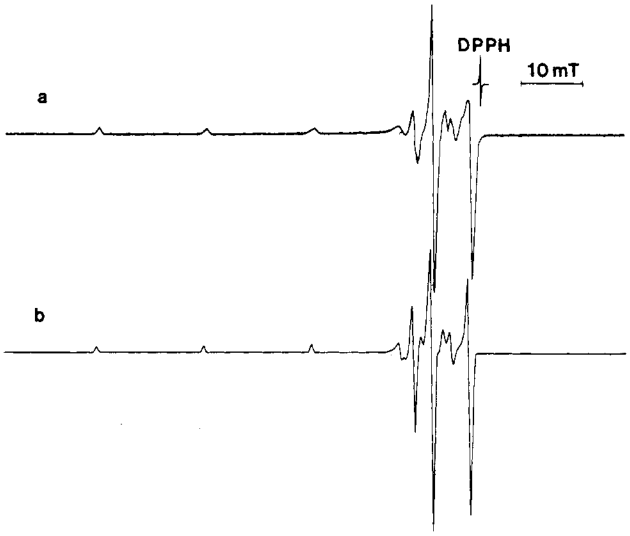

Figure 4. (a) X-band EPR spectrum for $PtCl_2\{^{63}Cu(acacP)_2\}$ in CH_2Cl_2/toluene (1:1) at 77 K and (b) its computer simulation.

cative of a nearly axially symmetric copper center. Simulation of the spectrum revealed the following parameters: $g_x = 2.061$, $g_y = 2.060$, and $g_z = 2.255$ with $A_x = 58$, $A_y = 81$, and $A_z = 561$ MHz for ^{63}Cu. The similarity of these values to those observed for copper bis(β-diketonate) complexes (Table VI) confirms that the square-planar Cu and Pt centers do not significantly interact. The fluid solution spectrum of $PtCl_2\{^{63}Cu(acacP)_2\}$ in toluene-CH_2Cl_2 consists of a single component (Figure 5) with g and hyperfine values ($g = 2.186$, $A(^{63}Cu) = 224.5$ MHz) very close to the average of those obtained from the frozen solution spectrum.

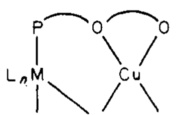

$L_nM = IrCl(CO)$
$L_nM = CuO_2CC_6H_4OCH_3$

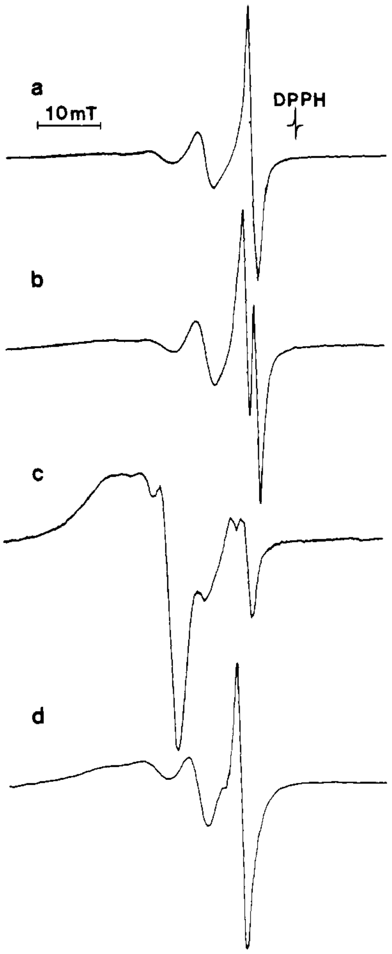

Figure 5. Fluid solution X-band EPR spectra of (a) $PtCl_2\{^{63}Cu(acacP)_2\}$ in toluene/CH_2Cl_2 (1:1), (b) $[IrCl(CO)\{^{63}Cu(acacP)_2\}SO_2]$ in toluene/CH_2Cl_2 (1:1), (c) $IrCl(CO)\{^{63}Cu(acacP)_2\}$ in CH_2Cl_2, and (d) $IrCl(CO)\{^{63}Cu(acacP)_2\}$ in 2-MeTHF.

In contrast, the X-band EPR spectrum of a frozen toluene-CH_2Cl_2 solution of $IrCl(CO)\{Cu(acacP)_2\}$ is broad and is poorly resolved. The principal features of the spectra of the ^{63}Cu-enriched complex at 9.1 GHz (X-band) (Figure 6a) and 35 GHz (Q-band) (Figure 6c) were approximately simulated (parts b and d of Figure 6) with $g_x = 2.038$, $g_y = 2.146$, and $g_z = 2.278$, and $A_x = 206$, $A_y = 103$, and $A_z = 314$ MHz, indicating a rhombic distortion about Cu(II). The low symmetry at the Cu site in the bimetallic complex is proposed to arise from coordination of an enolate oxygen of the β-diketonate chelate to Ir in an analogous manner to the structurally characterized Cu(I)Cu(II) complex $[Cu_2(acacP)_2(\mu\text{-}O_2CC_6H_4OCH_3)]$.[32] Such interactions are well-known for the other β-diketonate complexes[33,34] and would be geometrically quite comparable to the coordination of a methoxy group in complexes of the type $RuCl_2(o\text{-}Ph_2PC_6H_4OCH_3)_2$[35] and *trans*-$IrCl(CO)(o\text{-}Ph_2PC_6H_4OCH_3)_2$.[30] Three additional sharp features are present in the X-band spectrum and one feature in the Q-band spectrum at fields characteristic of the axial Cu(β-diketonate)$_2$ class of compounds. These species are relatively minor components of the solution although the sharpness of their absorptions in the $g_\perp$ region renders them readily detectable. We suggest that these other signals result from the presence of small amounts of square-planar Cu(II) species containing noninteracting

---

[32] Wrobleski, D. A.; Wilson, S. R.; Rauchfuss, T. B. *Inorg. Chem.* **1982**, *21*, 2114.

[33] Bullen, G. J.; Mason, R.; Pauling, P. *Inorg. Chem.* **1965**, *4*, 456.

[34] Cotton, F. A.; Elder, R. C. *Inorg. Chem.* **1965**, *4*, 1145.

[35] Jeffery, J. C.; Rauchfuss, T. B. *Inorg. Chem.* **1979**, *18*, 2658–66.

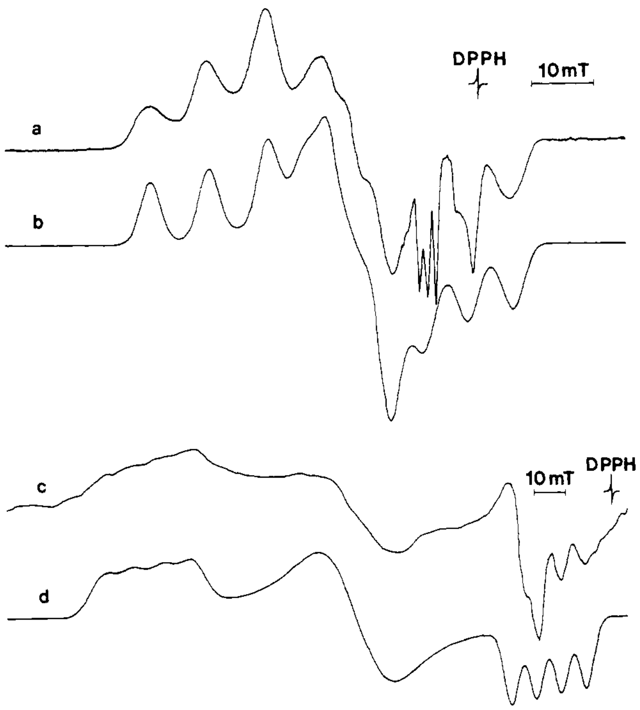

Figure 6. EPR spectra of IrCl(CO){^{63}Cu(acacP)$_2$} in CH_2Cl_2/toluene (1:1) at 77 K: (a) X-band experimental spectrum and (b) its computer simulation, (c) Q-band experimental spectrum, and (d) its computer simulation.

Cu and Ir moieties in equilibrium with a IrCl(CO){Cu(acacP)$_2$} complex containing enolate-bridged Cu and Ir atoms.

The spectrum observed for a fluid CH_2Cl_2 solution of IrCl(CO){^{63}Cu(acacP)$_2$} is considerably more complicated (Figure 5c) than the spectra of PtCl$_2${^{63}Cu(acacP)$_2$} and [IrCl(CO){^{63}Cu(acacP)$_2$}(SO$_2$)] (vide infra), and its major component ($g = 2.176$) is characterized by A(^{63}Cu) (Table VI), which is much smaller than the hyperfine splittings for the other binuclear species. In strongly coordinating solvents such as 2-MeTHF, the low-field peak disappears; the spectrum of such solutions (Figure 5d) is characterized by a ^{63}Cu hyperfine splitting similar to those for the noninteracting systems (parts and b of Figure 5). Taken collectively, these data suggest that in weakly coordinating solvents, IrCl(CO){Cu(acacP)$_2$} exists as an equilibrium mixture of species with and without a perturbed Cu center whereas coordinating solvents and SO_2 disrupt this interaction.

The X-band EPR spectrum of frozen solutions of [IrCl(CO){Cu(acacP)$_2$}SO$_2$] (Figure 7) is quite different from the precursor complex but closely resembles that of PtCl$_2${Cu(acacP)$_2$}. Since it is well established that SO_2 binds to *trans*-IrCl(CO)(PPh$_3$)$_2$[18] and we find that Cu(β-diketonate)$_2$ complexes do not detectably bind SO_2, these observations support the idea that coordination of SO_2 to the iridium(I) center in IrCl(CO){Cu(acacP)$_2$} disrupts a Ir$\cdots$Cu interaction, thereby permitting the Cu center to revert to pseudoaxial symmetry (eq 9). The complexity of the spectrum in the $g_\perp$ region indicates the presence of two EPR active species that may be a consequence of solvent coordination or, more likely, the presence of isomers as indicated in our ^{31}P NMR studies of IrCl(CO){Zn(acacP)$_2$}. Spectra similar to the Pt–Cu complex were observed for toluene and CH_2Cl_2 fluid solutions of [IrCl(CO){Cu(acacP)$_2$}SO$_2$] (Figure 5b), except that in these cases the high-field copper peak was split into a doublet.

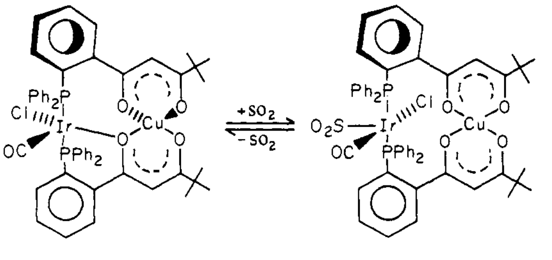

(9)

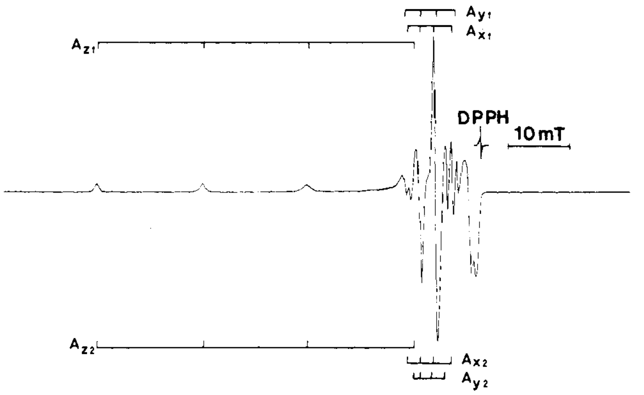

Figure 7. X-band EPR spectrum of [IrCl(CO){^{63}Cu(acacP)$_2$}SO$_2$] in CH_2Cl/toluene (1:1) at 77 K with bars representing the g and hyperfine values for two species derived by computer simulation.

The relative intensities of the two components of this doublet varied as a function of solvent, suggesting that the splitting was due to the presence of two different species and not superhyperfine coupling to a $I = {}^1/_2$ nucleus. The two species are assumed to arise from geometrical isomers akin to those characterized by ^{31}P NMR spectroscopy for [IrCl(CO){Zn(acacP)$_2$}SO$_2$]. Alternatively, the solution may contain differently solvated species whose rate of solvent interchange would be slow compared to the EPR time scale.

Discussion of EPR Data. The nuclear hyperfine structure in the frozen solution spectra consists of both isotropic (A_{iso}) and anisotropic components. For copper in the square-planar geometry, the isotropic component of the hyperfine interaction arises primarily from "core polarization" of inner-shell s orbital electron density by the unpaired spin density in valence d orbitals.[36] The anisotropic component can be largely attributed to the direct coupling of the unpaired d-electron spins with the nucleus. For the complexes studied in this work, the isotropic hyperfine splitting obtained from fluid solution data was found to be the average of the hyperfine coupling constants derived from the frozen solution data, $A_{iso} = {}^1/_3(A_x + A_y + A_z)$. The data allow the relative signs of the A_x, A_y, and A_z to be determined and allows one to calculate the components of the anisotropic hyperfine tensor, $A_x - A_{iso}$, $A_y - A_{iso}$, and $A_z - A_{iso}$.

For all of the complexes studied in this work, the magnitude of the principal components of the anisotropic hyperfine tensors are quite similar to the value of 320 MHz reported for ^{63}Cu(acac)$_2$.[37] By comparison with theoretically calculated coupling constants,[38] the numbers indicate that the unpaired spin density is of at least 50% d orbital character. However, to the extent that the **g** and hyperfine tensors are not coaxial, the hyperfine splittings measured from the frozen solution spectra will be less than the real hyperfine coupling constants. This occurs simply because in such situations the hyperfine splittings are not being measured along the principal directions of the hyperfine tensor but at angles to them that are related to the angles between the **g** and hyperfine tensor systems. Additionally the copper orbital contribution will be underestimated in proportion to the unpaired spin if there is any electron density in copper p orbitals because of the opposite signs of the contributions from p and d electrons to the hyperfine interaction.[38]

For IrCl(CO){Cu(acacP)$_2$} the isotropic hyperfine splittings are very much smaller than those found for the complexes featuring noninteracting metals. We assume that the core polarization and its isotropic component of the hyperfine splitting (~220 MHz) will be similar for all of these complexes since their d orbital spin density are all similar (vide supra). The diminished isotropic hyperfine splittings for IrCl(CO){Cu(acacP)$_2$} can be attributed to a modest rehybridization of copper. The lowering of symmetry

---

[36] Goodman, B. A.; Raynor, J. B. *Adv. Inorg. Chem. Radiochem.* **1970**, *13*, 135–362.

[37] Northern, T. M Ph.D. Dissertation, University of Illinois, Urbana, IL, 1976.

[38] Morton, J. R.; Preston, K. F. *J. Magn. Reson.* **1978**, *30*, 577–82.

of the copper site induced by the Ir–enolate interaction could allow the 4s orbital to mix to some extent with the molecular orbital containing the unpaired spin density. Since spin density in the 4s orbital produces a hyperfine coupling of opposite sign to that arising from core polarization, the 4s spin density can be estimated. Depending on whether the sign of A_{iso} is positive or negative (i.e., whether the magnitude of the interaction from the 4s spin density is greater than or less than that for core polarization), the 4s spin density is calculated as either 5.5% or 2% by comparing our values of +110 or +330 MHz with literature values.[38]

Acknowledgment. This research was supported by a generous grant from Dow Chemical Co. We thank Professor R. L. Belford for helpful discussions. NMR spectra were measured at the University of Illinois NSF Regional NMR Facility (NSF CHE 79-16100).

Registry No. *cis*-$PtCl_2(HacacP)_2$, 81141-53-9; $PtCl_2(COD)$, 12080-32-9; *cis*-$PdCl_2(HacacP)_2$, 81141-54-0; $PdCl_2(COD)$, 12107-56-1; *trans*-$IrCl(CO)(HacacP)_2$, 81157-62-2; $IrCl(CO)_2$(*p*-toluidine), 14243-22-2; *trans*-$RhCl(CO)(HacacP)_2$, 91312-15-1; $Rh_2Cl_2(CO)_4$, 14523-22-9; $PtCl_2\{Cu(acacP)_2\}\cdot 2CH_2Cl_2\cdot H_2O$, 91383-66-3; $PtCl_2\{Ti(acacP)_2Cl_2\}$, 91312-16-2; $PdCl_2\{Cu(acacP)\}$, 81141-52-8; $IrCl(CO)\{Cu(acacP)^2\}$, 91312-17-3; $IrCl(CO)\{Cu(acacP)_2\}SO_2$, 91327-60-5; $IrCl(CO)\{Zn(acacP)_2\}$, 91312-18-4; $Zn(acacP)_2$, 91312-19-5; $IrCl(CO)\{Zn(acacP)_2\}SO_2$, 91327-61-6; $IrCl(CO)(HacacP)_2SO_2$, 91327-62-7.

Reactions of Water and Ammonia with Bis(pentamethylcyclopentadienyl) Complexes of Zirconium and Hafnium

Gregory L. Hillhouse and John E. Bercaw*

Contribution No. 6875 from the Arthur Amos Noyes Laboratory of Chemical Physics, California Institute of Technology, Pasadena, California 91125.

Received August 4, 1983

Abstract: The propensity for the group 4B metal center to form extremely strong bonds with oxygen and nitrogen donors is often invoked as an important driving force in the reductions of carbon monoxide and dinitrogen with organometallic derivatives of these metals, e.g., $Cp^*_2ML_x$ ($Cp^* = \eta^5\text{-}C_5Me_5$; M = Ti, Zr, Hf). In order to assess some of the fundamental bonding properties of hydroxide, oxo, and amide ligands with bis(pentamethylcyclopentadienyl) derivatives of zirconium and hafnium, the reactivities of water and ammonia with several $Cp^*_2ML_x$ (M = Zr, Hf) complexes have been examined. Water reacts in a clean, stepwise manner with $Cp^*_2MH_2$ (M = Zr, Hf) to afford $Cp^*_2M(H)(OH)$, $(Cp^*_2MH)_2O$, $Cp^*_2M(OH)_2$, and finally $Cp^*_2M(OH)_2\cdot H_2O$. $Cp^*_2M(H)(Cl)$ yields $Cp^*_2M(OH)(Cl)$. $Cp^*_2MH_2$ reacts with $Cp^*_2M(OH)(X)$ (X = Cl, OH, H) to afford $Cp^*_2(X)M\text{–}O\text{–}M(H)Cp^*_2$. In all cases, conversion of a M–H bond to an M–O bond is accompanied by H_2 evolution. Similarly, ammonia reacts rapidly with $Cp^*_2MH_2$ to yield $Cp^*_2M(H)(NH_2)$ and H_2. Excess ammonia or $Cp^*_2MH_2$ do not react further, although exchange with free $^{15}NH_3$ is observed. $Cp^*_2Hf(H)(NH_2)$ reacts with H_2O to afford $Cp^*_2Hf(H)(OH)$ and NH_3, but not $Cp^*_2Hf(OH)(NH_2)$. Free water undergoes rapid proton exchange and slower oxygen exchange with the hydroxo derivatives. $(Cp^*_2ZrN_2)_2N_2$ reacts rapidly and cleanly with an equivalent of water to produce N_2 (3 equiv) and $(Cp^*_2ZrH)_2O$. Evidence in support of a stepwise oxidative addition of both O–H bonds via the intermediacy of $Cp^*_2Zr(H)(OH)$ is presented. ^1H and ^{17}O NMR spectra of these new compounds are also tabulated.

Introduction

The chemistry of the group 4B metals (Ti, Zr, Hf) in their higher oxidation states is dominated by the propensity of these metals to form extremely strong bonds with "hard" ligands such as O, N, F and Cl donors.[1] We have been interested in defining some of the fundamental bonding properties of such hard ligands with the zirconium and hafnium bis(pentamethylcyclopentadienyl) fragments, because these strong metal–ligand interactions are often invoked as important driving forces in reductions of carbon monoxide and dinitrogen with derivatives of $(\eta^5\text{-}C_5Me_5)_2M$ (M = Ti, Zr, Hf) (eq 1, 2).[2,3] Furthermore, it has been long recognized that essentially all $(\eta^5\text{-}C_5Me_5)_2ML_x$ compounds react vigorously with moisture to give soluble species, so that a systematic investigation of the water decomposition of $(\eta^5\text{-}C_5Me_5)_2ZrH_2$, $[(\eta^5\text{-}C_5Me_5)_2Zr(N_2)]_2(\mu\text{-}N_2)$, and related compounds seemed warranted. Finally, the observed stability of the hydrido amide complexes $(\eta^5\text{-}C_5Me_5)_2HfH(NHR)$ (R = Ph, tol) caused us to question whether the isoelectronic hydrido hydroxide complex $(\eta^5\text{-}C_5Me_5)_2HfH(OH)$ might be formed in reactions of water with $(\eta^5\text{-}C_5Me_5)_2HfH_2$.[4] Very few hydroxo hydride complexes are known, but they are considered to be important intermediates in "water splitting" reactions.[5,6]

$$(\eta^5\text{-}C_5Me_5)_2ZrH_2 + CO + H_2 \rightarrow (\eta^5\text{-}C_5Me_5)_2ZrH(OMe) \quad (1)$$

$$[(\eta^5\text{-}C_5Me_5)_2Zr(N_2)]_2(\mu\text{-}N_2) + 4HCl \rightarrow 2(\eta^5\text{-}C_5Me_5)_2ZrCl_2 + N_2H_4 + 2N_2 \quad (2)$$

There exists a large body of literature describing the interactions of water with cyclopentadienyl ($Cp \equiv \eta^5\text{-}C_5H_5$) complexes of Ti, Zr, and Hf,[7] with the earliest such study dating back to the first

---

(1) Wailes, P. C.; Coutts, R. S. P.; Weigold, H. "Organometallic Chemistry of Titanium, Zirconium, and Hafnium"; Academic Press: New York, 1974.

(2) (a) Manriquez, J. M.; McAlister, D. R.; Sanner, R. D.; Bercaw, J. E. *J. Am. Chem. Soc.* **1976**, *98*, 6733–35. (b) Manriquez, J M.; McAlister, D. R.; Sanner, R. D.; Bercaw, J. E. *Ibid.* **1978**, *100*, 2716–24. (c) Wolczanski, P. T.; Threlkel, R. S.; Bercaw, J. E. *Ibid.* **1979**, *101*, 218–20. (d) Wolczanski, P. T.; Bercaw, J. E. *Acc. Chem. Res.* **1980**, *13*, 121–27.

(3) Manriquez, J. M.; Sanner, R. D.; Marsh, R. E.; Bercaw, J. E. *J. Am. Chem. Soc.* **1976**, *98*, 3042–44.

(4) Hillhouse, G. L.; Bercaw, J. E. *Organometallics* **1982**, *1*, 1025–29.

(5) (a) Gillard, R. D.; Heaton, B. T.; Vaughan, D.. *J. Chem. Soc. A* **1970**, 3126–30. (b) Eady, C. R.; Johnson, B. F. G.; Lewis, J. *J. Chem. Soc., Dalton Trans.* **1977**, 838–44. (c) Chaudret, B. N.; Cole-Hamilton, D. J.; Nohr, R. S.; Wilkinson, G. *Ibid.* **1977**, 1546–57. (d) Johnson, B. F. G.; Lewis, J.; Raithby, P. R.; Zuccaro, C. *Ibid.* **1980**, 716–20. (e) Jones, R. A.; Wilkinson, G.; Colquohoun, I. J.; McFarlane, W.; Galas, A. M. R.; Hursthouse, M. B. *Ibid.* **1980**, 2480–87. (f) James, B. R.; Preece, M.; Robinson, S. D. "Catalytic Aspects of Metal Phosphine Complexes"; American Chemical Society: Washington, D. C., 1982; *Adv. Chem. Ser. No. 196*, pp 145–61. Also see ref 6.

(6) (a) Yoshida, T.; Ueda, Y.; Otsuka, S. *J. Am. Chem. Soc.* **1978**, *100*, 3941–42. (b) Yoshida, T.; Matsuda, T.; Okano, T.; Kitani, T.; Otsuka, S. *Ibid.* **1979**, *101*, 2027–38. (c) Yoshida, T.; Otsuka, S. "Catalytic Aspects of Metal Phosphine Complexes"; American Chemical Society: Washington, D. C., *Adv. Chem. Ser. No. 196*, pp 136–44. (d) Gargano, M.; Giannoccaro, P.; Rossi, M. *J. Organomet. Chem.* **1977**, *129*, 239–42.

(7) Leading references include: (a) Giddings, S. A. *Inorg. Chem.* **1964**, *3*, 684–87. (b) Samuel, E. *Bull. Chem. Soc. Fr.* **1966**, 3548–64. (c) Brainina, E. M.; Dvoryantseva, G. G.; Freidlina, R. Kh. *Dokl. Akad. Nauk SSSR (Engl. Transl.)* **1964**, 633–36. (d) Thewalt, U.; Kebbel, B. *J. Organomet. Chem.* **1978**, *150*, 59–66. (e) Guggenberger, L. J.; Tebbe, F. N. *J. Am. Chem. Soc.* **1976**, *98*, 4137–43. (f) Fronczek, F. R.; Baker, E. C.; Sharp, P. R.; Raymond, K. N.; Alt, H. G.; Rausch, M. D. *Inorg. Chem.* **1976**, *15*, 2284–89. (g) Reference 1 and citations contained therein. (h) Hunter, W. E.; Hrncir, D. C.; Vann Bynum, R.; Penttila, R. A.; Atwood, J. L. *Organometallics* **1983**, *2*, 750–755.